ELSEVIER

Earth and Planetary Science Letters 136 (1995) 17–30

EPSL

Biostratigraphic and magnetostratigraphic intercalibration of latest Cretaceous and Paleocene depositional sequences from the deep-water Basque basin, western Pyrenees, Spain

Victoriano Pujalte [a], Juan-Ignacio Baceta [a], Jaume Dinarès-Turell [b], Xabier Orue-etxebarria [a], Josep-Maria Parés [b], Aitor Payros [a]

[a] *Dpto. Estratigrafía y Paleontología, Universidad del Pais Vasco, Apartado 644, 48080 Bilbao, Spain*

[b] *Paleomagnetic Laboratory, Institute of Earth Sciences "Jaume Almera" CSIC, c / Martí i Franquès s / n., 08028 Barcelona, Spain*

Received 10 April 1995; accepted 7 August 1995

Abstract

Latest Cretaceous (Late Maastrichtian) and Paleocene depositional sequences from the deep-water Basque basin have been calibrated with published [1,2] and newly acquired magnetostratigraphic data. Sequences mostly consist of hemipelagic marls and limestones, and their relative ages are well constrained with planktic foraminifera. They accumulated during a phase of tectonic tranquillity and reduced clastic input into the basin, and therefore they can be attributed to eustatic sea-level changes with reasonable confidence.

On the basis of the planktic foraminifera zonation, a good match has been observed previously between the depositional sequences of the Basque basin and specific sea-level cycles of the 1988 version of the Exxon Global Cycle Chart (GCC) [3]. Here, a new attempt at correlation using their respective magnetostratigraphic data has failed to confirm such a match. The disagreements observed may indicate that, for the studied interval, (1) the current planktic foraminifera biostratigraphy lacks the necessary level of resolution to ensure synchrony between sequences of different basins, and/or (2) the magnetostratigraphy of the GCC needs to be revised. Whatever the case, the new findings lend support for some criticism on the use of the GCC for interregional correlations.

1. Introduction

The utility of modern sequence stratigraphy for global correlations remains controversial [4,5]. Such an application originally relied on two main assumptions: (1) that eustasy was generally a dominant factor in the development of depositional sequences, overprinting the effects of tectonics and sedimentary supply [6,7], and (2) that the Mesozoic and Cenozoic history of eustatic sea-level changes could be reconstructed and charted using data of well-studied basins around the world [8].

In relation to the first point, however, several workers have demonstrated that tectonics and sedimentary flux are factors of equal importance as eustasy in sequence development, being able to create sequences by themselves even in the absence of eustatic variations. Some changes through sequences may result largely from one single factor (i.e., eustatic- or tectonic-dominated), but most would de-

SSDI 0012-821X(95)00157-3

velop from the interplay of two or three of these variables. Moreover, it is often difficult to unravel the eustatic signature from the stratigraphic record because the stratigraphic architecture of the sequences is very similar independently of the particular factor(s) that caused them [9,10]. The Global Cycle Chart (GCC), which is based on the second assumption, has been criticized on the ground that the resolution of biostratigraphy is not sufficient to prove the synchrony between sequences of different basins [5].

However, the idea of simultaneous rises and falls of global sea level, particularly during non-glacial periods, is still appealing for both industrial and academic reasons. Additional efforts should therefore be made to prove or disprove the whole concept, searching for additional clues in the stratigraphic record. Such clues should preferentially be extracted from eustatic-dominated successions. Besides, the biostratigraphic age control of such successions should be carefully checked against magnetostratigraphy, since reversals of the geomagnetic field are one of the few geological events that are both synchronous and world-wide in scope.

The Basque basin offers an excellent opportunity to further this line of inquiry. This basin was a deep-water interplate trough flanked to the north (Aquitania), south (Iberia) and east sides by shallow shelf areas, and opening to the west into the Bay of Biscay (Fig. 1). Throughout the Late Maastrichtian and Paleocene, the sea transgressed the flanking shallow areas, leading to the development of extensive ramps or carbonate platforms [3,11,12]. That overall transgression also made it difficult for coarse-grained siliciclastics to reach the deep trough, which became the site of a hemipelagic limestone/marl type of sedimentation, with turbidites being mostly restricted to the base-of-slope area (Fig. 1). Depositional sequences have been identified in this succession that can be recognized basin wide, and they ensure very reliable lithological correlations between available sections, in many cases at bed-to-bed level ([12,13], and below).

Paleomagnetic studies have earlier been carried

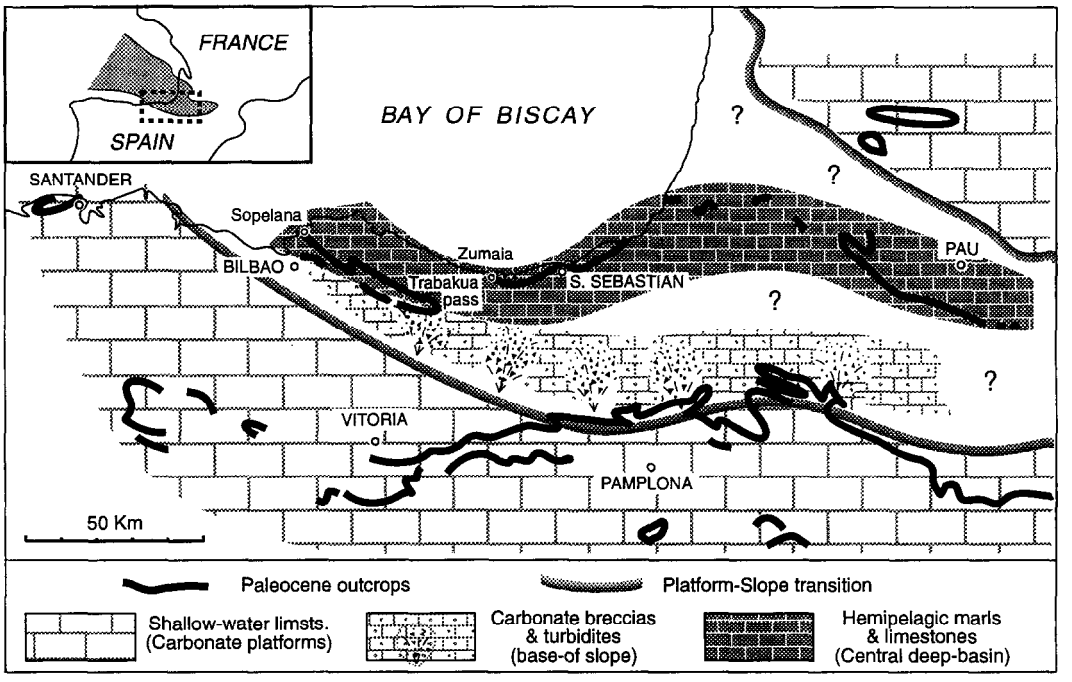

Fig. 1. Simplified Paleocene paleogeography of the western Pyrenees showing the main sedimentary domains that can be reconstructed from the overall facies distribution of available outcrops.

out successfully on two classical coastal cliff exposures of the Basque basin, Zumaia [1] and Sopelana [2]. These have now been supplemented with the analysis of the Trabakua pass section (location in Fig. 1). The paleomagnetic data of these three sections almost completely encompass the whole Late Maastrichtian–Paleocene interval, thus allowing a geomagnetic calibration of the sequences mentioned above. We will first discuss the new paleomagnetic data, and will then proceed to integrate them with previous information on sequences, biostratigraphy and magnetostratigraphy.

2. Magnetostratigraphy of the Trabakua pass section

2.1. Setting

The studied section is situated on the northern flank of the Biscay synclinorium, about 3 km to the north of the Trabakua pass itself (Fig. 1). It has been recently created by the enlargement of the local road Bi-140, and for that reason the rocks were still quite fresh at the moment of sampling, in the spring of 1994. From bottom to top it is composed of:

(1) 129 m of grey hemipelagic limestones and reddish to deep-purple marls, belonging to the Late Maastrichtian Zumaia–Algorri Formation [14]. As is distinctive in this formation, marl-dominated intervals alternate in the vertical profile of the Trabakua pass with others formed by limestone–marl rythmites. The same stacking pattern can be recognized basin wide, and it has been used by previous authors to subdivide the Zumaia–Algorri Formation into five laterally correlative members [15–17]. The formation conformably overlies a thick (1200 m) Campanian–Lower Maastrichtian flysch unit and is capped by the Cretaceous–Tertiary (K/T) boundary clay;

(2) 53 m of gray- and pink-colored hemipelagic limestones and marls, which embrace the whole Paleocene. A careful correlation with several other sections of the Basque basin has shown the occurrence of three meaningful hiatal surfaces within the Paleocene of the Trabakua pass (shown in the corresponding lithological logs by undulating heavy lines, see below). The extents of each of these hiatuses have been partly constrained with biostratigraphy, but even more accurately by assessing the number of missing beds with respect to the Zumaia section, the thickest and most complete of the basin [13];

(3) 4 m of dark-gray claystones (weathering out into reddish colors) which, unlike the remainder of the studied succession, is very poor in carbonate microfossils. Accordingly, it has been named the "Dissolution Interval" (DI) [18]. A strong negative excursion of $\delta^{13}C$, an isotopic event used by some authors as the position of the Paleocene–Eocene boundary, has been reported at the lower part of the DI in the Zumaia section [18];

(4) 50 m of gray hemipelagic limestones and marls, dated as earliest Eocene. These sediments are conformably overlain by a thick (> 2000 m) Lower–Middle Eocene flysch succession, which are the youngest Tertiary deposits preserved in the Biscay synclinorium.

2.2. Paleomagnetic sampling

The sampled portion of the section is composed of 9 m of purple marlstones, belonging to the uppermost (V) member of the Maastrichtian Zumaia–Algorri Formation; the whole 53 m of the Paleocene; and the lowest 25 m of the Eocene above the DI. Special care was taken to collect unweathered material and, whenever necessary, relatively long cores were drilled to avoid the exposed parts of the rocks. A total of 161 cores were collected from 92 stratigraphic levels using a portable gasoline powered drill machine, and they were oriented in situ with a magnetic compass. Average sampling spacing was slightly about 1 m. Beds are steeply dipping to the S–SW, the average dip direction and dip being 195/55. In the laboratory, core samples were cut in two to four standard specimens of 2.54 cm in diameter and 2.10 cm in length.

2.3. Paleomagnetic measurements and results

The natural remanent magnetization (NRM) was measured with a GM400 three-axis cryogenic magnetometer (CCL Ltd.). Stepwise thermal demagnetization was carried out by heating the samples in a TSD-1 Schondsted furnace. The intensity of the NRM was moderate to weak, generally about 5×10^{-4} A/m in the upper 15 m of the section, averaging

8×10^{-5} A/m in the middle one, and increasing again downsection, but showd values of up to 3×10^{-3} A/m in the Maastrichtian purple marlstones. Characteristic remanent magnetizations (ChRM) were computed by Principal Component Analysis [19] on the orthogonal demagnetization plots [20].

One to three specimens per sampling site were thermally demagnetized up to temperatures of 550–580°C with increasing 50° steps. Samples requiring further demagnetization were heated up to 640°C with 20° steps, for the intensity to decrease below the noise level of the magnetometer, or until an erratic behavior of the magnetization was observed. Typical examples of thermal demagnetization are illustrated in Fig. 2. A multicomponent character of the NRM is clear in the majority of the cases. A low-temperature component is unblocked below 250–300°C. This component has northerly declination and moderate to steep downward inclinations (about 60°) before rotating the bedding to the horizontal and becomes southerly directed with moderate to steep downwards inclinations after a tectonic correction has been applied (Fig. 2). This component is believed to represent a secondary recent overprint (present geomagnetic field direction). The gray marly limestones from the Eocene part of the section define an antiparallel component to the present-day field direction between temperatures of about 300 and 450°C (specimens TK17-1c and TK19-1d from Fig. 2). Thermal demagnetization above 450°C delineated a vector that decayed to the origin of the orthogonal diagram which is taken as the characteristic remanent magnetization (ChRM). This ChRM component has dual polarities and is believed to represent the primary magnetization. Some Paleocene reddish limestones display a single component magnetization after a small viscous component is removed at low temperatures (TK37-4b in Fig. 2). In other cases the ChRM is defined after the removal of the present-day component (TK56-1b in Fig. 2). It is important to note that samples that display a normal ChRM component also carry an antipodal reverse direction (TK68-1a and TK78-1b in Fig. 2) unblocked at lower temperature. In those cases, we have taken the highest temperature component (normal component) as the oldest one. Therefore, this component is used to compute the respective virtual geomagnetic pole (VGP). Since the opposite case does not seem to

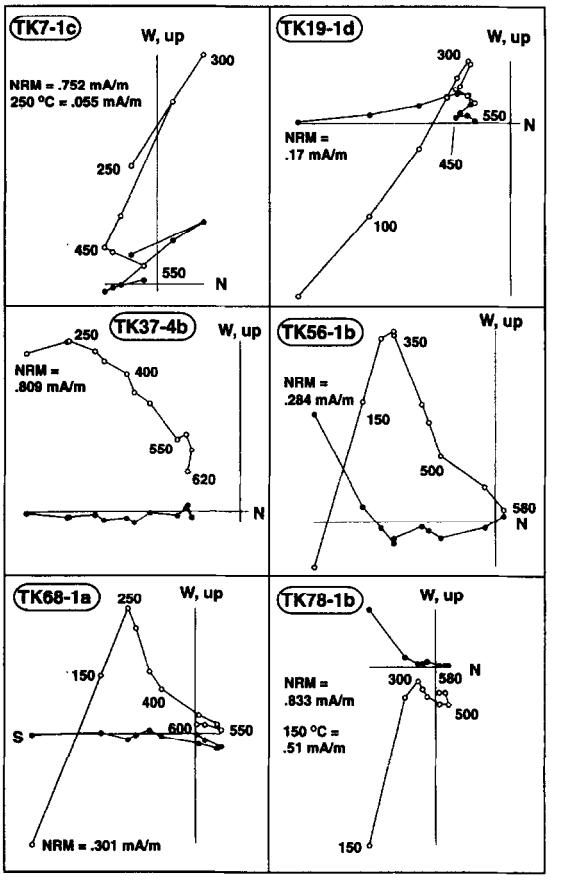

Fig. 2. Tectonic-corrected representative orthogonal projections of thermal demagnetization data from the Trabakua pass section. Open and closed symbols represent projections on the vertical and horizontal planes, respectively. Temperatures (in °C) are indicated for various points.

exist (reverse highest temperature ChRM and antipodal normal ChRM component) we may infer that this is due to (1) the fact that the normal Paleocene magnetozones are relatively short in time compared with the reversed magnetozones [21], and (2) the reversed magnetozones are interrupted by numerous short normal events (cryptochrons) of less than 30 kyr duration [21]. In such a scenario, samples deposited during a normal magnetozone will still block part of its ChRM in the opposite polarity corresponding to the field of the subsequent reverse magnetozone in a process similar to that described by Channel et al. [22], for ChRM residing in hematites in pelagic sediments from the Gubbio section (Italy).

Note that in the present case both components seem to be blocked in a magnetite-like mineral phase attending the unblocking temperature spectra, although this is not conclusive. Additional support for the general assumption comes from the fact that most of the section is reversely magnetized and also from biostratigraphic and sedimentologic evidence that points to a condensation of the series in the lowermost Paleocene (see also below) where the longest Paleocene normal magnetozones exists (chrons C28N and C29N lasting 1.233 and 0.821 Ma, respectively) [21].

Another thermal demagnetization behavior comes from samples collected slightly beneath the DI (see below), that display a southerly directed ChRM component but with positive polarity once the bedding has been restored to the horizontal. We interpret such cases as the result of a total overlap of the unblocking temperature spectra of the dual-polarity ChRM components described above and therefore we consider those samples as normally magnetized (see below). It is crucial to note that such cases occur in general just below or above normal magnetized samples and therefore we cannot rule out the possibility for those samples to reflect a transitional field.

The calculated ChRM [19] components before and after tectonic correction are plotted in Fig. 3. Samples exhibiting a downward and southerly direction after tectonic correction have been excluded. The computed mean direction [23] before tectonic correction ($D/I = 189/16$, $\alpha_{95} = 5.9$, $k = 6.5$) cannot represent any Cretaceous to present geomagnetic field, whereas once the tectonic correction has been applied the mean direction (all directions computed in the lower hemisphere, $D/I = 007/+39$, $\alpha_{95} = 4.2$, $k = 12$) conforms to that expected for the lower Tertiary. Thereafter both the coherency between observed and expected directions and the presence of normal and reversed polarities give confidence that the computed mean direction is primary. This magnetization probably resides in magnetite, although a hematite contribution with relatively low unblocking temperatures cannot be ruled out.

2.4. Magnetic stratigraphy

The calculated declinations and inclinations of the ChRM components have been used to derive the latitude of the virtual geomagnetic pole (VGP) (Fig. 4a). This parameter has been used as indicator of the polarity (normal polarity for positive VGP latitudes and reverse polarity for negative VGP latitudes) with the exception of those samples that exhibit downward and southerly directed directions which have been considered to reflect a normal polarity (shadowed portion in the polarity column from Fig. 4a) although the computed VGP has negative paleolatitudes.

The magnetic polarity sequence established at the Trabakua pass is characterized by the predominance

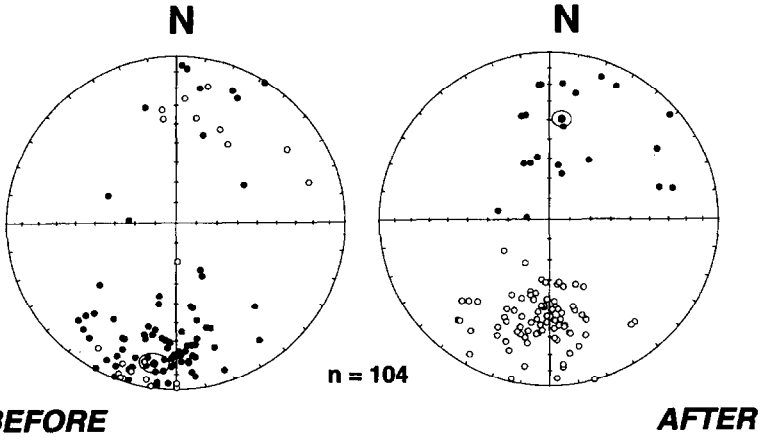

Fig. 3. Equal-area projections of the characteristics remanent magnetizations ChRM directions before and after tilt correction. Open and closed symbols represent projections on the upper and lower hemispheres, respectively. The mean direction (computed in the lower hemisphere) and its confidence oval are also shown.

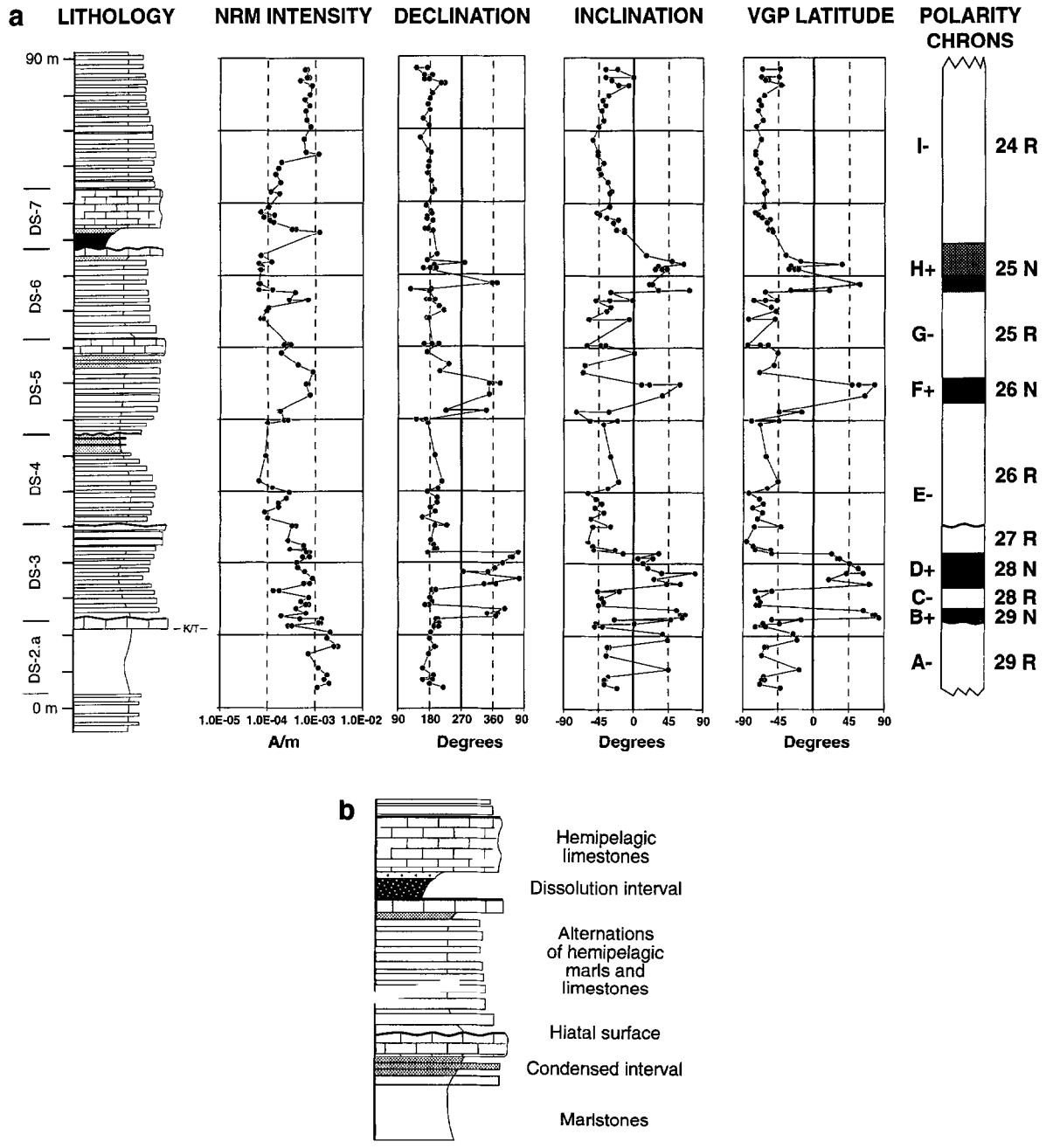

Fig. 4. (a) Stratigraphic variations of intensity, declination and inclination of ChRM vectors and computed VPG latitude, all of them plotted against the lithological log of the Trabakua pass section (DS-1 to DS-7 = depositional sequences; K/T = Cretaceous/Tertiary boundary; key to lithologies in b). Blank and solid polarities indicate reversed (negative) and normal (positive) polarities, respectively. Shadowed polarities probably also represent normal polarities. (b) Key to symbols on the lithological logs of Figs. 4a and 5.

of a reverse polarity with short normal intervals which define a total of 9 magnetozones (A − to I − in Fig. 4a, the upper and lower boundary of the younger and older magnetozones, respectively, not defined). Correlation with the standard Geomagnetic Polarity Time Scale (GPTS) [21] is relatively straightforward for the two uppermost normal magnetozones. Thus, chron H + is attributed to C25N mainly on the basis of its position relative to the $\delta^{13}C$ negative shift: in several DSDP holes the top of C25N occurs a few meters below that isotopic excursion [24]; at the Trabakua pass, the top of H + is not sharply defined (shadowed portion in the polarity column of Fig. 4a), but it must be situated between 1.5 and 4 m below the inferred location of the isotopic shift [18]. As for F +, its situation amid the planktic foraminifera biozone of *P. pseudomenardii* leaves little doubt about its equivalence with C26N.

Correlating the remaining chrons is faced with a few uncertainties, that can be surmounted by comparison with other sections. As mentioned above, planktic foraminifera data and detailed lithological correlations demonstrated the existence of three hiatuses in the Paleocene of the Trabakua pass. The middle hiatus comprises the upper part of the *E. trinidadensis* biozone plus the *M. uncinata* and *M. angulata* biozones ([13], and below). Chron C27N, which in the Zumaia section occurs during that time interval [1], is therefore missing in Trabakua. For that reason, the portions of E − above and below that hiatal surface have been respectively ascribed to

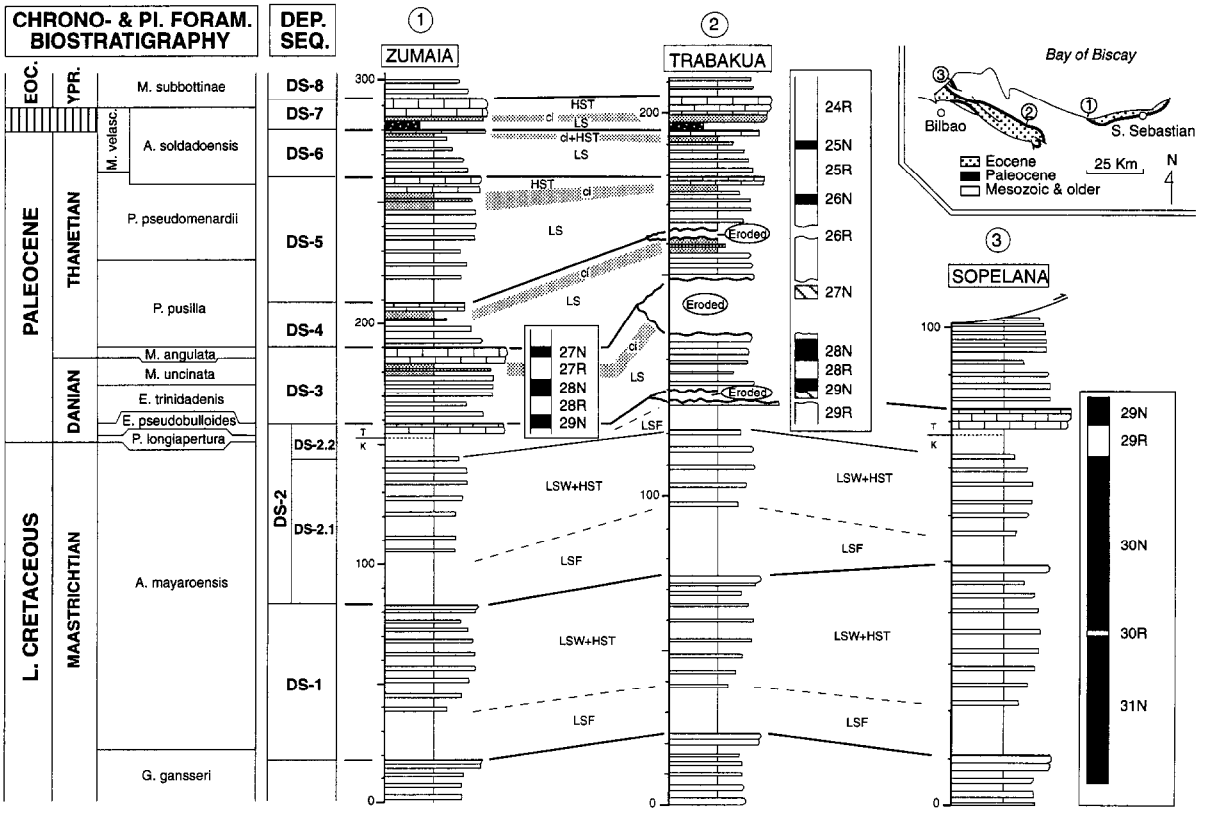

Fig. 5. Simplified lithological logs of three Late Maastrichtian and Paleocene sections of the Basque basin for which paleomagnetic information is currently available (shown within insets to the right of the logs). Key to lithological symbols on Fig. 4b. In order to facilitate the visual comparison among the three logs, their vertical scales have been changed and, in the Trabakua section, the thickness of missing rocks (hiatuses) has been taken into account. Note also that much fewer beds are illustrated in the logs than actually exist in the field. Planktic foraminifera zonation after Orue-etxebarria [3,29].

C26R and C27R (Fig. 4a). Finally, magnetozones D + and B + occur in the lower part of the Paleocene succession of Trabakua, and they must correspond respectively to C28N and C29N, the only two remaining normal polarity chrons of the Early Paleocene. It should be also noted in Fig. 4a that the lower limit of chron B + coincides with the lower Paleocene hiatal surfaces, a fact that explains the reduced thickness of C29N at Trabakua (1.5 m) compared to Zumaia (9 m) [1].

3. Sequence stratigraphy

Seven depositional sequences have been recognized in the study area for the Late Maastrichtian–Paleocene interval, which Pujalte et al. [12] named DS-1 to DS-7 successively. The same coding is used in this report (Fig. 5). In all cases, their estimated time span falls into the 3rd-order range of Vail et al. [25]. Each individual sequence has been traced laterally from the shallow-water carbonates of the north Iberian platform, through the breccias and calcarenites of the base-of-slope apron flanking it, into the hemipelagic accumulation of the central deep basin (Fig. 1). In addition to that, but only within the hemipelagic stacks of the central part of the basin, DS-2 can be subdivided into two subsequences, 2a and 2b.

Both in the shallow-water carbonate platform and in the base-of-slope apron (Fig. 1), the depositional sequences are bounded by important erosional and/or non-depositional surfaces [3,12]. By contrast, such discontinuities are usually much less important in the hemipelagic stacks flooring the central parts of the basin [13]. These basinal deposits can be accurately dated with planktic foraminifera, and they happen to be the most favorable ones for the analysis of paleomagnetism. They offer therefore a unique opportunity to cross-correlate the depositional sequences with both the planktic foraminifera and the geomagnetic scales.

3.1. Lithological characterization of the depositional sequences

Lithological stacking patterns vary in detail between depositional sequences, but for simplicity they can be conveniently divided in two main groups: one group includes sequences composed of two parts (DS-1 and -2, mostly Late Maastrichtian); the other group comprises those in which a three-fold division can be recognized (DS-3 to -7, Paleocene). The physiography of coeval shallow settings was ramp-like during the Late Maastrichtian [26], but oscillated between a distally steepened ramp and a rimmed platform during the Paleocene [3,12], and that is the most likely cause for the different facies architectures of the two groups. Flooding events on the ramps were more or less continuous because of the near uniform slopes of these settings. Hence the homogeneous lithologies of the contemporary basinal accumulations (i.e., the upper parts of DS-1 and -2). However, the nearly flat tops of Paleocene plat-

Table 1
Summary features of late Maastrichtian depositional sequences of the Basque basin (DS-1 and -2)

PARTS OF THE SEQUENCE	LITHOLOGICAL PARAMETERS			INTERPRETATION
	Gross lithological character	Relative sedimentation rate	Type of turbidites (in Zumaia section)	
Upper	Limestone-dominated	Lowest	Mixed (carbonate siliciclastic)	Lowstand wedge + Highstand (LSW + HST)
Lower	Marlstone-dominated	Highest	Mixed (carbonate siliciclastic)	Lowstand fan (LSF)

form margins were temporarily drowned during phases of fast sea-level rise [12], and the carbonate and siliciclastic fluxes into the basin were both reduced. These transgressive phases of the shelf are represented in the basin by the condensed intervals observed in the middle parts of DS-3 to -7.

The constituent parts of the sequences in both groups have been delineated with the help of the following interrelated criteria (Tables 1 and 2): (1) long-term vertical changes of the bulk carbonate/clay ratios, which result in an alternation of marlstone-dominated and limestone-dominated intervals. The basin-wide development of these alternations was first demonstrated for DS-1 and -2 [15–17], and later on for the other sequences [13]; (2) variations of sedimentation rates, estimated from the thicknesses of the stratification cycles (i.e., couplets and bundles, thought to be tuned to Milankovitch frequencies [13,27]), which are the building blocks of the sequences; and (3) variations in the frequency and/or the composition of turbidite intercalations, criteria that can be applied solely in the Zumaia section, which is the only one with a substantial proportion of thin-bedded turbidites.

Comparison between the different sections confirms that the three hiatuses of the Paleocene succession at the Trabakua pass can be traced laterally into important erosional discontinuities in the slope apron and shallow-water platform facies. They represent therefore sequence boundaries that are indicative of erosional phases that locally affected the basin floor at the onset of lowstand periods. Otherwise, sequence boundaries are expressed in the field by a sudden increase in both sedimentation rates and marl/limestone ratios. Smit et al. [27] concluded that the high sedimentation rates of the lower parts of both DS-2a and -2b resulted from a simultaneous increase in the fluxes of both carbonate and terrigeneous clays, and that the marly-dominated parts of these sequences were developed at times of the highest rates of carbonate supply into the basin. The same reasoning can be extended to the Paleocene sequences [13].

Taking into account the current models concerning sea-level fluctuations and deep-sea sedimentation (e.g., [28]), and observations made at the contemporaneous north Iberian shelf and base-of-slope settings [12], the recurring pattern just outlined can be satisfactorily explained in terms of sequence stratigraphy. The two or three parts recognizable in the sequences have been ascribed therefore to different sea-level stands (Tables 1 and 2). Thus, the lower parts of the sequences are considered lowstand deposits because of their position above sequence boundaries and their relative enrichment in fine-grained terrigeneous materials: as sea level fell during a lowstand period the

Table 2
Summary features of Paleocene depositional sequences of the Basque basin (DS-3 to -7)

PARTS OF THE SEQUENCE	LITHOLOGICAL PARAMETERS			INTERPRETATION
	Gross lithological character	Relative sedimentation rate	Type of turbidites (in Zumaia section)	
Upper	Limestone-dominated	Intermediate	Carbonate	Highstand (HST)
Middle	Intermediate or marlstone-dominated	Lowest	Do not occur	"Condensed interval" (Basinal equivalent of the shallow-water TST)
Lower	Marlstone-dominated	Highest	Mixed (carbonate siliciclastic)	Undiferentiated lowstand (LS = LSF+LSW)

coastline would have migrated basinwards, making it easier for siliciclastic silts and clays to reach the basin. The primary productivity would also be simultaneously enhanced, both processes jointly increasing sedimentation rates [27,28].

Refloodings of the shelf during sea-level rises reversed the process, leading in all cases to a decline in deep-sea sedimentation rates. The limestone-dominated character of the upper part of the sequences is clear proof that such decline was mainly due to a more or less effective storing of fine grained terrigeneous sediments on carbonate ramps (Late Maastrichtian) or platforms (Paleocene). The parallel drop in primary productivity was compensated in part by carbonates being shed off these shallow settings, as evidenced by the occurrence of platform-derived carbonate turbidites in the Zumaia section.

3.2. Biostratigraphic calibration of depositional sequences

Planktic foraminifera are generally abundant and reasonably well preserved in the Basque basin, and have been used for dating the studied succession. Current results are shown in the left-hand side of Figs. 5 and 6. In doing this, we have followed the zonation worked out for this particular basin by

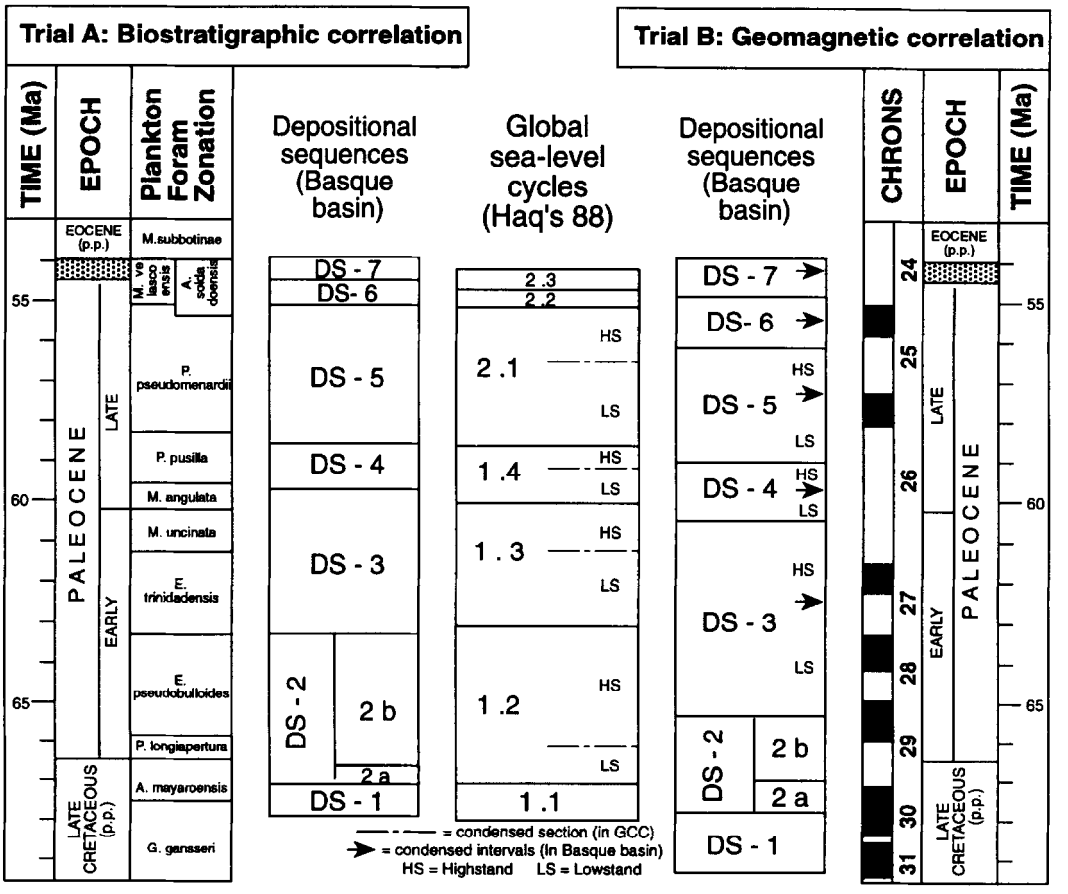

Fig. 6. Two independent attempts to correlate the depositional sequences recognized in the Basque basin and the 3rd-order cycles of sea-level change of the GCC. In trial A the correlation is solely based on their respective planktic foraminifera zonations; in trial B, on their paleomagnetic calibration.

Orue-etxebarria [29] (see also appendix 1 in [3]). But for some minor details, that zonation is similar to one of Stainforth et al. [30], which was used to calibrate the GCC, which makes the comparison between the two relatively easy (but see below). Thus, all but one of the recognizable biozones are named after their defining taxon (i.e., *A. mayaroensis*, *P. pusilla*, etc.), their bases being placed at the first appearance datum (FAD) of the corresponding species. The only exception to this rule is the biozone of *M. velascoensis*, the base of which is situated at the last appearance datum (LAD) of *P. pseudomenardii*.

3.3. Magnetostratigraphic calibration of depositional sequences

The lithological expressions of the depositional sequences in three of the hemipelagic sections of the Basque basin from which paleomagnetic information does exist are shown in Fig. 5. Again, it must be reiterated that the correlation between these sections is very reliable, for most of the succession even at the bed-to-bed level [13,15–17]. Information can thus be confidently transferred between these sections, allowing paleomagnetic calibration of the sequences. This calibration is particularly good for the Lower Paleocene, for which data are available from at least two sections. The Upper Maastrichtian and Upper Paleocene have been calibrated solely on one data set, from the Sopelana [2] and Trabakua sections (this study), respectively.

Based on this information, DS-1 and -2a were developed entirely during the time span of chrons 31N to 30N. A better precision can be offered for DS-2b, the LSF of which occurred during C29R, while its HST deposits were laid down during the lower part of C29N (however, the data from the three sections concur with previous studies, e.g., [31–33], in placing the position of the K/T boundary towards the upper part of C29R). A even more calibration precise can be attained for DS-3: its lower boundary is placed at the middle of C29N, the lower part of this chron being eroded at Trabakua; its LS deposits encompass both the reversed and normal parts of C28; and its condensed interval and HST deposits are situated within C27R and C27N, respectively. The eroded interval at Trabakua comprises most of C27R, the whole of C27N, and probably a small part of C26R (Fig. 5).

Data from Trabakua finally indicate that the deposition of DS-4 occurred in its entirety during the lower part of C26R; DS-5 encompasses the remainder of C26R, C26N and the lowermost part of C25R, and DS-6 spans the upper part of C25R, C25N and the lower part of C24R, the normal polarity chrons being situated in both sequences immediately below their condensed intervals. Lastly, DS-7, the youngest of the studied sequences, occurs within the lower part of C24R.

4. A comparison of regional and global cyclicities

The accuracy of the GCC may be under discussion, but it is the best approximation so far available about the history of 3rd-order sea-level changes. As a test of its reliability for the Late Maastrichtian–Paleocene interval, we have compared the results from the Basque basin with those from the same interval of the GCC. This comparison has been carried out through two independent sets of correlations, one based on the planktic foraminifera zonation, the other making use of the geomagnetic polarity scale.

The first of these attempts is facilitated by the fact that the majority of the boundaries of both the depositional sequences and sea-level cycles considered in this study seem to have occurred at, or near to, the FAD of zonal index species. The resulting correlation suggests that each of the sequences of the Basque basin can be ascribed to a specific 3rd-order cycle of the GCC, and vice versa (trial A in Fig. 6). The match is not so good, however, in the second case (trial B in Fig. 6). Four main discrepancies have been identified, which are discussed below:

(1) The lower boundaries of DS-1 and of cycle 1.1 occur, both in the Basque basin and in the GCC, immediately below the FAD of *A. mayaroensis*. Therefore, they appear at about the same level in trial A of Fig. 6. However, the lower boundary of DS-1 has been found to occur in the Basque basin within C31N, whereas in the GCC the base of cycle 1.1 is placed at the lower part of C30N. In the geomagnetic correlation the offset between these two boundaries is about 1.5 Ma. (Fig. 6).

The reason for this disparity is clearly the fact that the GCC places the FAD of *A. mayaroensis* too high. Hubert and Watking [33] have shown that, although it is diachronic, this datum is never so young: it usually occurs within chron 31N, and it can even be found towards the middle part of C31R in the southern high-latitudes.

(2) The nominal planktic foraminifera zonations of DS-2 and cycle 1.2 are similar, spanning from the middle part of *A. mayaroensis* to the end of *E pseudobulloides*. According to the paleomagnetic calibration, however, their respective temporal distributions barely overlap.

(3) Both in the Basque basin and in the GCC the lower boundaries of DS-3 and of cycle 1.3 roughly coincide with the FAD of *E. trinidadensis* (Fig. 6A). However, in the Basque basin this bioevent is thought to have occurred within C29N, whereas in the GCC it is plotted near the C27R/C28N reversal.

The reasons for these two disagreements is connected with the contrasting opinions that exist between specialists concerning the geomagnetic position of the base of the *E. trinidadensis* biozone (marked by the FAD of the zonal species). For instance, in the classic paper by Berggren et al. [34], this biohorizon is placed at the top of C28N, a datum also adopted in the GCC. However, at least two micropaleontologists, each working independently in different areas of Spain, reported the FAD of *trinidadensis* on the lower part of C29N. (i.e., Smit, in [35], and Orue-etxebarria, in [2] and this report). In a later paper by Berggren [36], in which he questioned Smit's findings and reasserted his own position, it became clear that different taxonomic concepts ot the species *trinidadensis* do persist among micropaleontologists.

As a result, very different solutions are obtained for this particular interval in each of the trials shown in Fig. 6. If the biostratigraphic correlation is made using Smit's/Orue-etxebarria's taxonomic concept of *trinidadensis*, the boundaries of both DS-2/DS-3 and cycles 1.2/1.3 would be situated at about the same position, suggesting a contemporaneous event. However, the geomagnetic correlation indicates that the age of the DS-2/DS-3 boundary is about 2 Ma older than that of cycles 1.2/1.3 in the GCC. Even more worrying is the fact that the sea-level fall that created the lower boundary of DS-3 would have taken place amid a highstand phase of the GCC; whereas the opposite would have happened, with respect to the Basque basin, with the sea-level drop that marks the base of cycle 1.3 in the GCC (Fig. 6).

(4) The bases of DS-6 and of cycle 2.2 are situated at the bottom of the *M. velascoensis* biozone, a biohorizon defined by most micropaleontologists by the LAD of *P. pseudomenardii* (see above). Yet, according to the paleomagnetic data from the Trabakua pass, the lower boundary of DS-6 is placed towards the middle–upper part of C25R, while that of cycle 2.2 is shown in the GCC in the upper part of C24R (Figs. 4 and 6).

This final discrepancy implies an offset of nearly 1 Myr and, in all likelihood, it is a consequence of the time-transgressive character of the LAD of *P. pseudomenardii*, as already recognized by Blow [37].

5. Concluding discussion

Depositional sequences have been delineated in the Late Maastrichtian and Paleocene sediments of the western Pyrenees, that can be traced laterally from the shallow north Iberian platform into the deep-water Basque basin [3,12,13]. They can be considered good examples of eustatic-dominated sequences, since contemporaneous tectonics in the area was subdued, and siliciclastic flux into the basin was negligible. In the central parts of the Basque basin they are developed within a nearly continuous stratigraphic succession largely made up of hemipelagic marls and limestones. These sediments contain a wealth of well-preserved planktic foraminifera that permit a reliable age dating of the sequences. Other important groups of microfossils, notably nannoplankton [15], deep-water microbenthic foraminifera [18], and palynomorphs, are also present although their study has been so far restricted to the lower and upper boundaries of the Paleocene. Furthermore, the predominantly carbonate nature and the fine-grained textures of these sediments make them suitable for paleomagnetism. Consequently, the geomagnetic reversal history can be readily derived. In short, the Basque basin reveals itself as an important reference area in which it has been possible to intercalibrate depositional sequences, probably of eustatic origin,

with both biostratigraphically meaningful fossils and magnetostratigraphy.

These results have made it clear that, for the studied interval, the planktic foraminifera and geomagnetic scales are not well intercalibrated in the GCC. It is not surprising, therefore, that the comparison between information gathered in the Basque basin with that compiled in the 1988 version of the GCC leads to equivocal results: if only planktic foraminifera zonation is taken into account, a reasonably good correlation can be established between the depositional sequences of this basin and specific 3rd-order cycles of the GCC; such a good match cannot be duplicated, however, when the correlation is attempted using their respective magnetostratigraphies.

However, biostratigraphic correlation alone is not a proof of synchrony, because at least some of the planktic foraminifera datum planes of the studied interval are demonstrably time-transgressive [33,37]. The synchrony cannot be checked with the magnetostratigraphy of the GCC either, because of its incorrect intercalibration with the planktic foraminifera scale. Indeed, this claim should only be considered fully justified when comparisons can be made between sequences directly calibrated with magnetostratigraphy. For this purpose, the calibration achieved in the Basque basin may eventually prove useful for the Late Maastrichtian–Paleocene interval.

These findings may detract from the credibility of the GCC in its present status, but not necessarily invalidate the whole concept behind the global chart. They only reinforce the view, already advanced by previous authors, that much research will still be needed to accurately constrain the history of past global sea-level changes.

Acknowledgements

Funds for this study were provided by the Basque Country University (research project UP 121.310-BE 233/93), and the DIGIT (research projects-0457 and PB91-0096). We thank both institutions for their economic support. Thanks are extended to three anonymous referees for their helpful reviews of an earlier version of this paper. [*RV*]

References

[1] W.M. Roggenthen, Magnetic stratigraphy of the Paleocene. A comparison between Spain and Italy, Mem. Geol. Soc. Ital. 15, 73–82, 1976.

[2] C. Mary, M.G. Moreau, X. Orue-etxebarria, E. Apellaniz and V. Courtillot, Biostratigraphy and magnetostratigraphy of the Cretaceous/Tertiary Sopelana section (Basque Country), Earth Planet. Sci. Lett. 106, 133–150, 1991.

[3] V. Pujalte, S. Robles, A. Robador, J.I. Baceta and X. Orue-etxebarria, Shelf-to-basin Palaeocene palaeogeography and depositional sequences, western Pyrenees, north Spain, in: Sequence Stratigraphy and Facies Associations, H.W. Posamentier et al., eds., Int. Assoc. Sedimentol. Spec. Publ. 18, 369–395, 1993.

[4] R.M. Carter, S.T. Abbot, C.S. Fulthorpe, D.W. Haywick and R.A. Henderson, Application of global sea-level and sequence-stratigraphic models in Southern Hemisphere Neogene strata from New Zealand, in: Sedimentation, Tectonics and Eustasy, D.I.M. Macdonald, ed., Int. Assoc. Sedimentol. Spec. Publ. 12, 41–65, 1991.

[5] A.D. Miall, Exxon global cycle chart: An event for every occasion?, Geology 20, 787–790, 1992.

[6] R.M. Mitchum, P.R. Vail and S. Thompson III, Seismic stratigraphy and global changes of sea level, Part 2: the depositional sequence as a basic unit for stratigraphic analysis, in: Seismic Stratigraphy Applications to Hydrocarbon Exploration, C.E. Payton, ed., AAPG Mem. 26, 53–62, 1977.

[7] P.R. Vail, R.M. Mitchum and S. Thompson III, Seismic stratigraphy and global changes of sea level from coastal onlap, in: Seismic Stratigraphy Applications to Hydrocarbon Exploration, C.E. Payton, ed., AAPG Mem. 26, 63–97, 1977.

[8] B.U. Haq, J. Hardenbol and P.R. Vail, Mesozoic and Cenozoic chronostratigraphy and cycles of sea-level change, in: Sea-Level Change: An Integrated Approach, C.K. Wilgus et al., eds., SEPM Spec. Publ. 42, 71–108, 1988.

[9] W.E. Galloway, Genetic stratigraphic sequences in basin analysis I: architecture and genesis of flooding-surface bounded depositional units, AAPG Bull. 73, 125–142, 1989.

[10] W. Schlager, Accommodation and supply - a dual control on stratigraphic sequences, Sediment. Geol. 86, 111–136, 1993.

[11] J.C. Plaziat, Late Cretaceous to Late Eocene palaeogeographic evolution of southwest Europe, Palaeogeogr. Palaeoclimatol. Palaeoecol. 36, 263–320, 1981.

[12] V. Pujalte, J.I. Baceta, A. Payros, X. Orue-etxebarria and J. Serra-Kiel, Late Cretaceous–Middle Eocene Sequence Stratigraphy and Biostratigraphy of the SW. and W. Pyrenees (Pamplona and Basque Basins, Spain), 118 pp., GEP/IGCP 286 Field Seminar Guide-Book, Basque Country Univ., Bilbao, 1994

[13] V. Pujalte, J.I. Baceta, X. Orue-etxebarria and A. Payros, The Paleocene of the Basque Country, W. Pyrenees, Spain: Facies and Sequence development in a deep-water, starved basin, in: Mesozoic and Cenozoic Sequence Stratigraphy of

European Basins, P.C. de Graciansky., ed., SEPM Spec. Publ., in press.

[14] B. Mathey, El Cretácico Superior del Arco Vasco, in: El Cretácico de España, Univ. Complutense Madrid, pp. 111–135, 1982.

[15] J.A. Burnett, W.J. Kennedy and P.D. Ward, Maastrichtian nannofossils biostratigraphy in the Biscay region (southwestern France, northern Spain), Newslett. Stratigr. 26, 145–155, 1992.

[16] K.G. Macleod and W.N. Orr, The taphonomy of Maastrichtian inoceramids in the Basque region of France and Spain and the pattern of their decline and disappearance, Paleobiology 19, 235–250, 1993.

[17] P.D. Ward and W.J. Kennedy, Maastrichtian Ammonites from the Biscay Region (France, Spain), Paleontol. Soc. Mem. 34 [suppl. J. Paleontol. 67(5)], 1–58, 1993.

[18] J.I. Canudo, G. Keller and E. Molina, Planktic foraminiferal turnover and $\delta^{13}C$ isotopes across the Paleocene–Eocene transition at Caravaca and Zumaya, Spain, Palaeogeogr. Palacoclimatol. Palaeoecol. 114, 75–100, 1995.

[19] J.L. Kirschvink, The least-squares line and plane and analysis of paleomagnetic data, Geophys. J.R. Astron. Soc. 62, 699–718, 1980.

[20] J.D.A. Zijderveld, A.C. demagnetization of rocks: analysis of results, in: Methods in Paleomagnetism, D.W. Collinsonet et al., eds., pp. 254–286, Elsevier, Amsterdam, 1967.

[21] S.C. Cande and D.V. Kent, A new geomagnetic polarity time scale for the Late Cretaceous and Cenozoic, J. Geophys. Res. 97(B10), 13,917–13,951, 1992.

[22] J.E.T. Channel, R. Freeman, F. Heller and W. Lowrie, Timing of diagenetic haematite growth in red pelagic limestones from Gubbio (Italy), Earth Planet. Sci. Lett. 58, 189–201, 1982.

[23] R. Fisher, Dispersion on a sphere, Proc. R. Soc. London A 217, 295–305, 1953.

[24] D.K. Pak and K.G. Miller, Paleocene to Eocene benthic foraminiferal isotopes and assemblages: implications for deepwater circulation, Paleoceanography 7, 405–422, 1992.

[25] P.R. Vail, F. Audemard, S.A. Bowman, P.N. Eisner and C. Perez-Cruz, The stratigraphic signatures of tectonics, eustasy and sedimentology - an overview, in: Cycles and Events in Stratigraphy, G. Einsele, W. Ricken and A. Seilacher, eds., pp. 617–656, Springer, Berlin, 1991.

[26] M. Floquet, La plateforme nord-Castillane au Crétacé supérieur (Espagne). Arrière-pays ibérique de la marge passive basco-cantabrique. Sédimentation et vie, Thesis, Univ. Bourgogne, Dijon, 925 pp., 1991.

[27] J. Smit, W.G. Ten Kate, A. Sprenger and A. Nederbragt, Sequence stratigraphy and cyclestratigraphy of the Cretaceous–Tertiary boundary in the Basque basin, in: Latest Cretaceous–Early Eocene Sedimentation in the Deep-Water Basque Basin, V. Pujalte et al., pp. 43–45, Field-trip Guide Book Int. Symp. Sequence Stratigraphy European Basin, Univ. Bourgogne, Dijon, 1992.

[28] B.U. Haq, Sequence stratigraphy, sea-level change, and significance for the deep sea, in: Sedimentation, Tectonics and Eustasy, D.I.M. Macdonald, ed., pp. 3–40, Int. Assoc. Sedimentol. Spec. Publ. 12, 1991.

[29] X. Orue-etxebarria, Los foraminíferos planctónicos del Paleógeno del sinclinorio de Bizkaia (corte de Sopelana-Punta Galea), Parte 1, Kobie 13, 175–249, 1983.

[30] R.M. Stainforth, J.L. Lamb, H. Luterbacher, J.H. Beard and R.M. Jeffoods, Cenozoic planktonic foraminiferal zonation and characteristic index forms, 425 pp., Univ. Kansas Paleontol. Contrib. 62, 1975.

[31] W. Alvarez, M.A. Arthur, A.O. Fisher, W. Lowrie, I. Premoli-Silva and W.M. Roggenthen, Upper Cretaceous–Paleogene magnetic stratigraphy at Gubio, Italy. Geol. Soc. Am. Bull. 88, 383–388, 1977.

[32] W. Lowrie and W. Alvarez, Late Cretaceous geomagnetic polarity sequence: detailed rock and paleomagnetic studies of the Scaglia Rossa limestone at Gubbio, Italy, J.R. Astron. Soc., 51, 561–581, 1977.

[33] B.T. Hubbert and D.K. Watkins, Biogeography of Campanian–Maastrichtian calcareous plankton in the region of the Southern Ocean: paleogeographic and paleoclimatic implications, Am. Geophys. Union Antarct. Res. Ser. 56, 31–60, 1992

[34] W.A. Berggren, D.V. Kent and J.J. Flynnn, Paleogene geocronology and chronostratrigraphy, in: The Chronology of the Geological Record, N.J. Snelling, ed., Geol. Soc. London, Mem. 10, 141–195, 1985.

[35] J.J. Groot, R.B.G. de Jonge, C.G. Langereis, W.G.H.Z. ten Kate and J. Smit, Magnetostratigraphy of the Cretaceous–Tertiary boundary at Agost (Spain), Earth Planet. Sci. Lett. 94, 385–397, 1989.

[36] W.A. Berggren, Comments on the paper "Magnetostratigraphy of the Cretaceous–Tertiary boundary at Agost (Spain)" by J.J. Groot, R.B.G. de Jonge, C.G. Langereis, W.G.H.Z. ten Kate and J. Smit, Eath Planet. Sci. Lett. 95, 183–185, 1989.

[37] W.H. Blow, The Cainozoic Globigerinida. A study of the morphology, taxonomy, evolutionary relationships and stratigraphical distribution of some Globigerinida (mainly Globigerinacea), 1413 pp., Brill, Leiden, 1979.